

POLYMER GRAPHENE NANOCOMPOSITES

Ahmed A. Abdala

Department of Chemical Engineering, The Petroleum Institute, Abu Dhabi, UAE
Authors' e-mails: aabdala@pi.ac.ae

ABSTRACT

The discovery of graphene in 2004 was followed by development of new methods for production of bulk quantities of modified graphene sheets. This with the combination of the extraordinary physical properties of graphene and the ability to disperse in various polymer matrices has led to emerge of a new era of polymer nanocomposites. This presentation reviews the different methods for production of chemically and thermally modified graphene sheets and their use in polymer nanocomposite with emphasis on our research work. Two polymer-graphene nanocomposites will be discussed in details. In the first nanocomposite, graphene is dispersed into a polar polymer, polymethyl methacrylate (PMMA). In such a nanocomposite where graphene is homogeneously dispersed into the polymer matrix, incorporation of graphene sheets has resulted in significantly improved mechanical electrical and thermal stability properties at very low loading of graphene, e.g. 0.05%. In the second, nanocomposite, graphene is dispersed into a nonpolar polymer, polyethylene (PE) matrix. In this later case, the poor dispersion of graphene into the nonpolar matrix yielded less significant enhancement in the mechanical, electrical, and thermal stability properties. Different attempts to improve the dispersion of graphene into PE such as using solvent mixing and functionalization of PE are also presented.

INTRODUCTION

Polymers have a range of attractive products such as low density, softness, elasticity, high toughness, ease of processing, corrosion resistance, electrical and chemical insulating properties. However, many specialty and advanced applications requires other added properties such as strength and stiffness, dimensionally stability, electrical, and thermal conductivity, thermal stability, flame retardancy, and diffusion resistance. One way to enhance the properties of polymers to meet the need of these special applications is incorporation of filler into the polymer matrix, i.e. forming polymer composites. In particular, polymer nanocomposites which include incorporation of nanosize fillers into polymer matrix can enhance mechanical properties, thermal stability, electrical and thermal conductivity, and barrier properties of polymers. Examples of nanofillers include Layered silicate (clay), nanosize carbon black and carbon fibers, carbon nanotubes, and graphene.

Graphene is a single layer of carbon atoms arranged in a honeycomb lattice which represents the 2-D carbon allotrope. Graphene is considered as the mother of all carbon based materials of all other dimensionality, e.g. the 0-D buckyminster, the 1-D carbon nanotube, and the 3-D graphite (Geim, 2007). Although graphene has been known since 1947, attempts to its experimental isolation was faced with experimental difficulties and misbelieve that it will be thermally unstable due to its low thermal stability due to its atomic thin structure. Geim and Novoselov has provide the first demonstration for successful isolation of graphene (Novoselov, 2004). This discovery has awarded them the 2010 Nobel prize in Physics.

Graphene has a number of unique properties that are very interesting for both fundamental studies and future applications. The surface area of graphene is 2626 m²/g. The mechanical properties of graphene are second to none. It has a measured tensile strength of 130 GPa, 100 times the strength of steel (Lee, 2008). The modulus of defect free graphene is 1.2 TPa which is 6 times the modulus of steel (Lee, 2008). The electrical and thermal transport properties of graphene are very unique. Graphene has room temperature electrical conductivity of 6x10³ S/m (Du, 2008) and thermal conductivity of 5x10³ W/m.K (Balandin, 2008). Single layer graphene is very transparent as it only absorbs 2.3% of incident light (Nair, 2008).

Graphene was initially isolated from graphite using the micromechanical method. Nowadays, graphene is produced using both bottom-up and top-down methods. Bottom-up methods build graphene sheets from compounds that include carbon. These methods include carbon vapor deposition (CVD), arc-discharge, epitaxial growth of SiC, self-assembly, and reduction of CO₂ (Kim, 2010). These methods typically provide small scale production of high quality and large size graphene sheets. These methods produce monolayer and multiple layer graphene suitable for electronic applications and fundamental studies. On the other hand, top-down methods separate graphene from directly from graphite or graphite derivative. These methods are suitable for "large scale" production of small size pure or chemically modified graphene suitable for applications that require large graphene quantities, e.g. polymer nanocomposites. Examples of the top-down methods include the micromechanical cleavage method, direct sonication of

graphite, Electrochemical method, supercritical CO₂ exfoliation of graphite, super acid dissolution of graphite, solvothermal reduction of graphite oxide (GO), chemical reduction of graphite oxide, and thermal exfoliation/reduction of graphite oxide.

Currently, the most promising methods for large scale production of graphene are based on the exfoliation and reduction of GO. GO was first prepared over 150 years ago by Brodie (Brodie, 1859). Analogous to graphite, which is composed of stacks of graphene sheets, GO is composed of graphene oxide sheets stacked with an interlayer spacing between 6 and 10 Å depending on the water content.

The GO is built of pristine aromatic “islands” separated from each other by aliphatic regions containing epoxide and hydroxyl groups and double bonds as shown in Fig. 1 (Lerf, 1998). GO has C/O atomic ratio of 2/1.

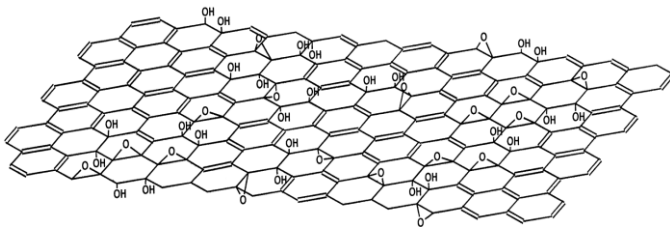


Fig.1. Proposed chemical structure of GO (Lerf, 1998)

The thermal exfoliation GO leads not only to separation of the graphene oxide sheets but also to reduce their oxygen content such that the C/O atomic ratio increases to about 10/1. This reduction process is necessary to restore the electrical properties of graphene as GO is electrically nonconductive but thermally reduced graphene (TRG) is highly conductive (MacAllister, 2007).

Polymer nanocomposite was one of the first areas that benefited from the discovery of graphene. In the first polymer graphene nanocomposite, Stankovich et. al. demonstrated that electrically conductive polystyrene (PS) can be made with a very low loading of chemically modified graphene (Stankovich, 2006). As shown in Fig. 2, PS-graphene nanocomposite percolates at a very low loading of chemically reduced graphene, i.e. 0.1 vol.%. Moreover, very high conductivity of 2.5 S/m was achieved with a loading of 2.5 vol.%.

Ramanathan et. al. also reported substantial improvement of the mechanical and thermal properties of polymethyl methacrylate (PMMA) with the addition of 1 wt.% of thermally reduced graphene (Ramanathan, 2008). The level of improvement in the mechanical properties (tensile strength and young’s modulus) is greater than the improvement by incorporation of 1 wt.% of SWCNT and expanded graphite as shown in Fig 3. They also observed an increase in glass transition temperature of 25° C with addition of 0.01 wt.% of functionalized graphene sheets (FGS). FGS is what we currently call TRG. However, these results remain

controversial as the increase in modulus is above the theoretical maximum as predicted by the Mori-Tanaka theory assuming infinitely large graphene sheets (Kim, 2010).

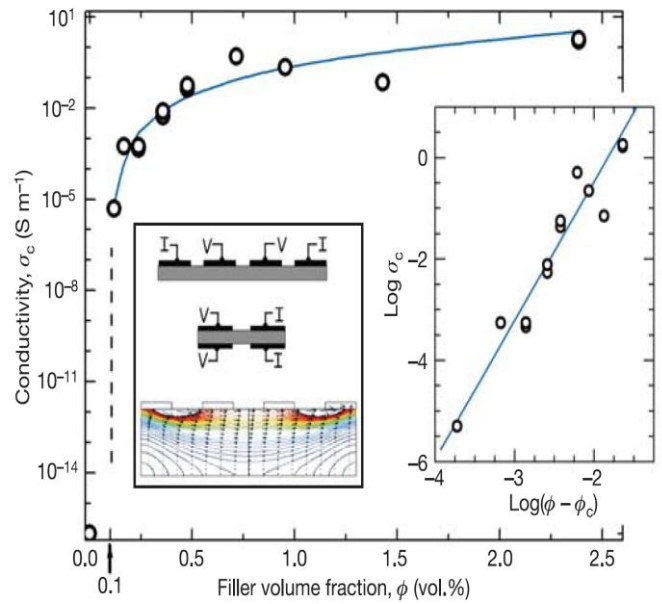


Fig.2. Electrical conductivity of polystyrene-graphene composite as function of graphene loading. (Stankovich, 2006)

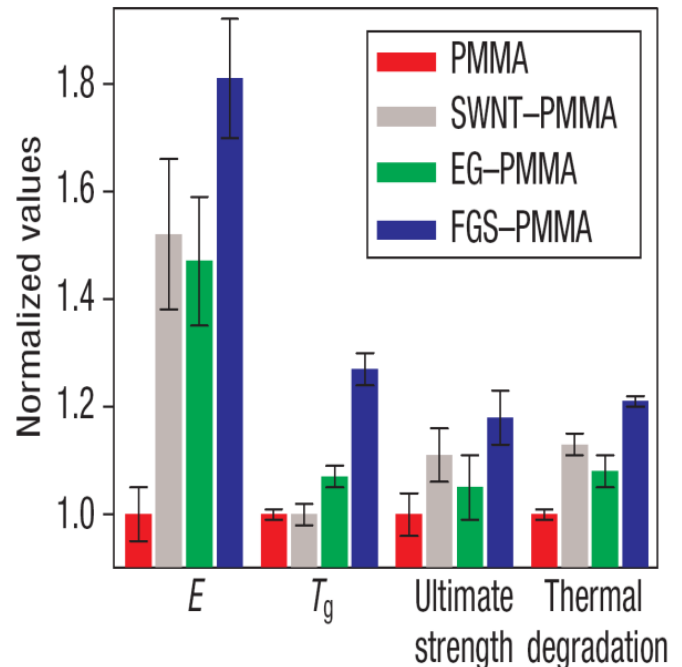


Fig.3. Mechanical, thermal, and Tg properties of PMMA composites with 1% SWNT, EG, and FGS (Ramanathan, 2008)

In this article, we describe the different routes for production of graphene with focus on the thermal exfoliation method and discuss few examples of their applications in polymer nanocomposites to improve the mechanical and electrical properties of polar and nonpolar polymers.

EXPERIMENTAL METHODS

Materials:

Natural flake graphite (-10 mesh, 99.9%, Alfa Aesar), Sulfuric Acid (95-97%, J.T. Bakers), Hydrochloric Acid (37%, Reidel- deHaen), Hydrogen Peroxide (30% solution, BDH), Potassium Permanganate and Sodium Nitrate (Fisher Scientific) are used as received. Commercial LLDPE resins, Affinity PE was obtained from the Dow Chemical Co. PE is a low-density PE copolymer of ethylene and octene (24 wt % octene content, density: 0.87 g/cm³, melt flow index: 5 g/10 min at 190 °C). Its weight (M_w) and number (M_n) averaged molecular weight are 201 and 67 kg/mol, respectively. The same PE, but grafted with MA (PE-MA, 0.8 wt % MA content) was also provided by the Dow Chemical Co. MA grafting was conducted in reactive extrusion with peroxides. M_w and M_n of PE-MA are 176 and 71 kg/mol, respectively. For TRG synthesis, natural flake graphite (-10 mesh, 99.9%) was purchased from Alfa Aesar.

Methods

Preparation of TRG

Graphite is oxidized using Staudenmaier method (Staudenmaier, 1898) as follows: graphite (5 g) is placed in ice-cooled flask containing a mixture of H₂SO₄ (90 ml) and HNO₃ (45 ml). Potassium chlorate (55 g) is added slowly to the cold reaction mixture. The reaction is stopped after 96 h by pouring the reaction mixture into deionized water (4 L). 5% HCl solution is used to wash the produced graphite oxide (GO) until no sulfite ions are detected. The mixture is then washed with water till no chloride ions are detected. GO is dried in a vacuum oven over night.

TRG is produced by simultaneous exfoliation/reduction of GO by rapid heating at 1000 °C in a tube furnace under flow of nitrogen for 30 s.

Nanocomposite Preparation

PE-TRG and functionalized PE-TRG composites with TRG loading from 0.5 wt.% to 3 wt.% are prepared by melt and solvent blending methods. In melt blending, PE and PE functionalized with maleic anhydride are blending with TRG at 180 °C in DACA microcompounder at 200 rpm speed for 8 minutes under N₂ purge. In solvent blending method, PE and PE-MA are dissolved in toluene refluxed at 110° C. TRG dispersion in toluene is mixed with PE toluene solution and stirred. The composite is solvent casted over heated plate 70-80° C.

Nanocomposite Characterization

Wide-angle X-ray diffractograms of graphite, GO, and TRG were obtained using a Bruker-AXS (SIEMENS)

D5005 X-ray diffractometer (CuK α radiation, 45kV and 40 mA) in the 2 θ range of 5 – 30° at scan rate of 0.02 °/s.

Scanning Electron Microscope (e-SEM, FEI Quanta 250) was used to study the morphology of TRG. TRG samples for SEM imaging were prepared by applying the powder directly to a carbon adhesive tape.

Transmission electron microscopy (TEM) was used to investigate the dispersion of TRG in different PE samples. Composite films embedded in an epoxy matrix (TRA-BOND 2115, Tra-Con) were microtomed (Leica Ultracut) at -90 °C into 85-100 nm thick slices using a diamond knife and transferred onto 400 mesh copper grids.

The degree of crystallinity of PE was determined by differential scanning calorimetry (DSC, TA Instruments Q1000). 5-10 mg of thin films was loaded into non-hermetic aluminum pans. Scanning was performed from -100 °C to 250 °C at the rate of 10 °C/min.

dc surface resistance of the composite films was measured with an 11-probe meter (PRS-801, Prostat). In order to ensure sample uniformity, geometric averages of the resistance measured from 3-4 different spots from each side of the films are reported.

Tensile stiffness of the composites was evaluated with Rheometrics Solids Analyzer (RSA II, TA Instruments). 3-4 mm wide strips cut from the solvent cast or compression molded films were mounted between the film fixtures of RSA II. Tensile deformation at 0.0005 /s was applied to the specimen and static Young's modulus was determined from the slopes of stress-strain responses of the composites at 0.5-1.5 % strain.

RESULTS AND DISCUSSION

Graphene Synthesis and Characterization

The morphology of the as prepared and dispersed TRG is examined using SEM and TEM as shown in Fig. 4. The fluffy aggregated and unlayered structure of TRG is evident in the SEM images, Fig. 4-a. The aggregation of the TRG as shown by the SEM images is expected for the as prepared TRG which was never dispersed in a liquid. On the other hand, the TEM image of TRG (Fig. 4-b) reveals that TRG is composed of thin and large sheets with paper-like structure. Large volume expansion upon exfoliation is clearly shown in Fig 4-c.

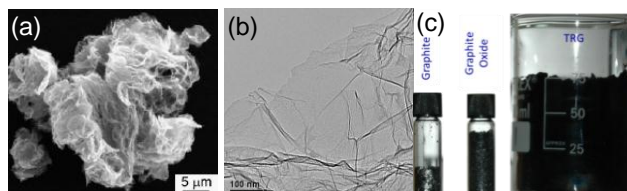


Fig.4: SEM image (a) and TEM Image (b) of TRG and electronic image showing the volume of 0.5 g of graphite, GO, and TRG (c).

The structural changes due to oxidation of graphite and exfoliation of GO is followed by XRD. Fig. 5 shows the

diffraction patterns for graphite, GO, and TRG. The diffraction pattern for graphite has a strong 002 peak at $2\theta = 26.4$ corresponding to the interlayer d-spacing of 0.335 nm. On the other hand, GO pattern shows the shift of the 002 peak to at $2\theta = 11.4$ indicating expansion of the interlayer spacing to 7.4 nm. Alternatively, TRG diffraction pattern does not show any diffraction peaks confirming the complete exfoliation of the reduced graphene layers.

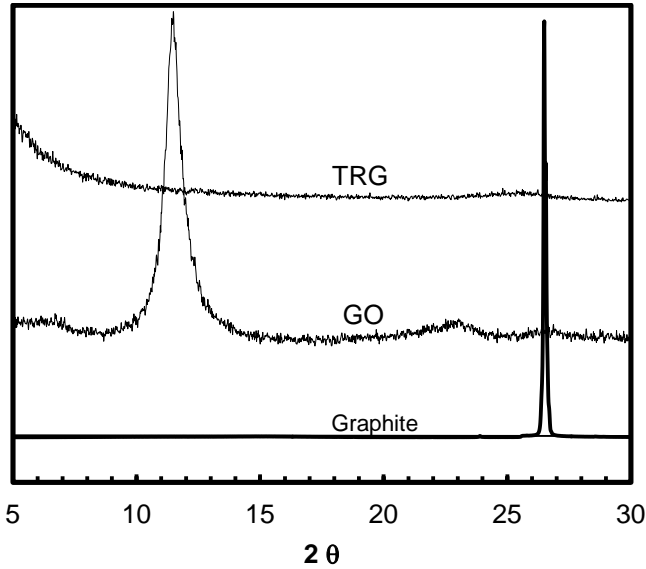


Fig. 5: XRD diffraction pattern of graphite, GO, and TRG.

Effect of Blending Method and PE Functionalization on Composite Morphology

The morphology of the nanocomposites is examined with TEM. Based on TEM micrographs, the role of PE functionalization and blending method on the dispersion of TRG is discussed in the next few sections.

Electron micrographs of melt blended PE and PE-MA containing 1 wt % TRG are provided in Fig. 6. Unlike fully isolated, single graphene sheets blended in solution (Fig. 7a and b), complete exfoliation is rarely observed for the melt compounded TRG/PE (Fig. 6a and b). In Fig. 6a and 6, areas highly concentrated with graphene stacks are distinguished from regions which lack graphene suggesting local concentration fluctuation. In melt compounding, graphene dispersion could not be improved by MA grafting on PE. In contrast to TRG layers well exfoliated in solvent blended PE-MA (Fig. 6c and d), melt processed samples appear predominantly phase separated (Fig. 7c and d). Note that the morphology of melt compounded TRG/PE is distinguished from that of solvent blended TRG in un-functionalized PE. While TRG aggregates formed after solvent mixing with PE show some degree of inter-particle connectivity (Fig. 7a and b), aggregates in melt blended PE are mostly isolated from one another (Fig. 6). These morphological differences may explain the observed trend in the electrical

conductivity of solvent and melt blend samples as will be discussed later.

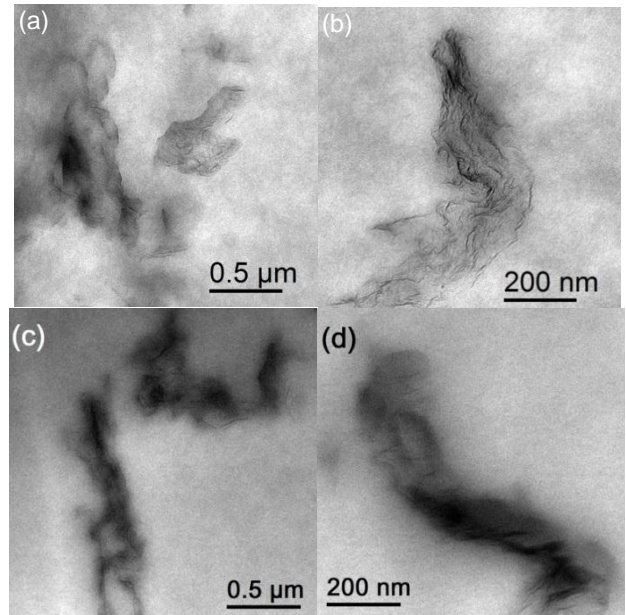


Fig.6. TEM micrographs of 1 wt.% TRG melt blended with PE (a, b) and PE-MA (c, d)

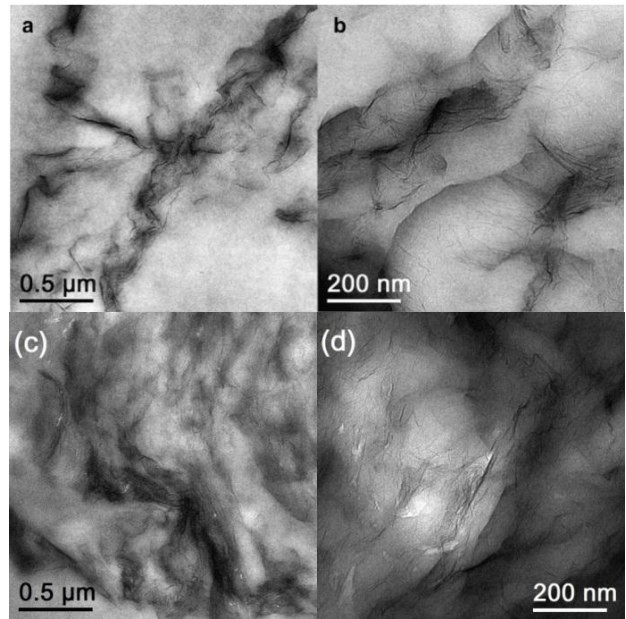


Fig.7. TEM micrographs of 1 wt.% TRG solvent blended with PE (a, b) and PE-MA (c, d)

Effect of Blending Method and Polymer Functionalization on Mechanical Properties

Different loading of TRG was incorporated into PE and PE-MA via melt and solvent compounding. The increase in Young's modulus for composite samples is shown in Fig. 8. For all composite samples, the modulus is higher

than that of pure polymer. Moreover, the increase in Young's modulus increases with TRG loading irrespective of the blending method and polymer type. However, the modulus improvement is more significant for solvent blended samples. The moduli for PE-MA samples are higher than those for the unfunctionalized samples for the same solvent blending method. These results are consistent with the morphology of the composite samples observed by TEM as discussed in the previous section.

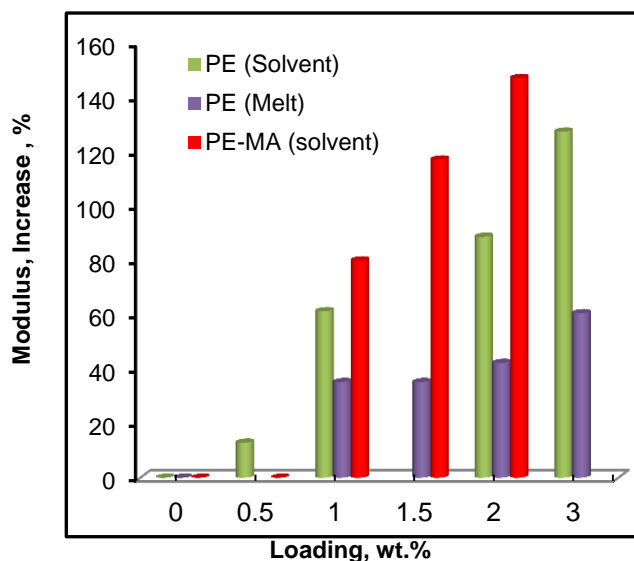


Fig. 8: increase in the modulus for PE-TRG and PE-MA-TRG composites with different TRG loading and blending methods.

The mechanical properties of semi-crystalline polymers including PE can be affected by the degree of crystallinity. Crystallinity in LLDPE and TRG composites was estimated by DSC measurements. Crystallinity of PE was 16% for both solvent cast and melt pressed films and was not appreciably influenced by either graphene dispersion or functionalization with MA. Therefore, reinforcement with graphene is solely responsible for the improved tensile stiffness of the composites.

Effect of Blending Method and Polymer Functionalization on Electrical Conductivity

Sample spanning pathways for electrical conduction can be formed via percolation of graphene in the polymer matrix. Surface resistance of PE and PE-MA composite samples with different loading of TRG blended by melt and solvent blending is shown in Fig. 9. As shown in the figure, addition of TRG decreases the surface resistance regardless of blending method or polymer functionalization. However, for all TRG loadings, the surface resistance of solvent blended samples is lower than that of the melt blended samples. This is consistent with the morphology of the solvent and melt blended samples. TRG loading required for electrical percolation for solvent blended samples, both PE and PE-MA, is about 0.5 wt.% (0.2 vol.%). In contrast, the percolation

loading for melt blended samples is about five times higher, i.e. 2.5 wt.% (1.0 vol.%)

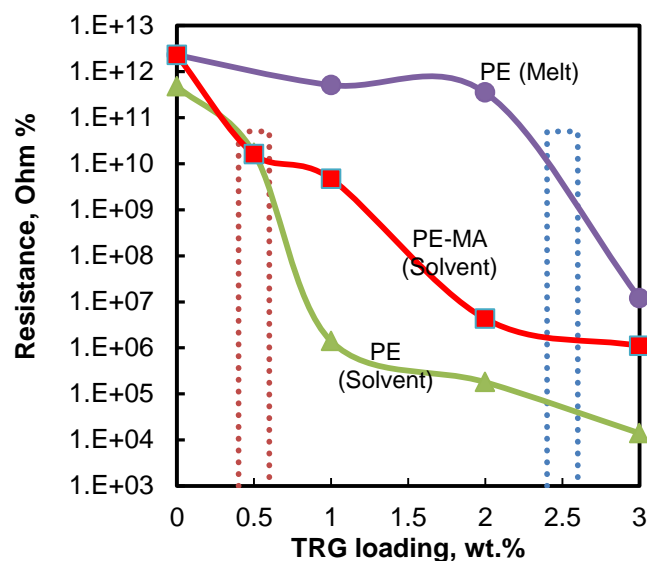


Fig. 9: Electrical resistance for PE-TRG and PE-MA-TRG composites with different TRG loading and blending methods.

A rather negative influence of PE functionalization on conductivity improvement is observed for PE-MA composites. In Fig. 9, a greater decrease in electrical resistance by TRG incorporation was achieved with PE than PE-MA for solvent blended samples. Even with seemingly better dispersion from TEM analysis, TRG in PE-MA resulted in higher electrical resistance than for TRG in PE throughout the entire concentration.

CONCLUSIONS

In this study, we investigated the effect of blending method and polyethylene functionalization on the dispersion of TRG into the polymer matrix and the resulted mechanical properties and electrical conductivity. We find that the melt blending method failed to disperse TRG into neither PE nor the functionalized PE-MA samples. On the other hand, solvent blending methods provided composites with well dispersed TRG into both PE and PE-MA samples. Moreover, maleic anhydride functionalization of PE, improved the dispersion of TRG compared to the unfunctionalized samples.

Incorporation of TRG into PE and PE-MA samples improves the stiffness of the composite samples as expressed by Young's modulus. The level of improvement is consistent with the quality of TRG dispersion into the PE and PE-MA samples.

The electrical conductivity of the composite samples indicates that the threshold for electrical percolation is highly dependent on the blending method. Solvent blended samples percolates at TRG loading of 0.5 wt.% which is five times higher than the percolation threshold

for melt blended samples. On the other hand, contrary to the dispersion quality observed by TEM, solvent blended PE-MA composite samples have higher electrical resistance than PE composite samples at all TRG loading.

Acknowledgement

The author Appreciate the contribution of Professor Chris Macosko research group at Department of Chemical Engineering and Materials Science, University of Minnesota. Financial support from the Abu Dhabi-Minnesota Institute for Research Excellence (ADMIRE) is acknowledged.

REFERENCES

Brodie, B. C. 1859. On the Atomic Weight of Graphite. *Philos. Trans. R. Soc. London* 149:249–259.

Balandin, A. A., S. Ghosh, W. Bao, I. Calizo, D. Teweldebrhan, D., F. Miao, and C. N. Lau. 2008. Superior Thermal Conductivity of Single-Layer Graphene. *Nano Letters* 8: 902-907.

Du, X., I. Skachko, A. Barker, and E. Y. Andrei. 2008. Approaching Ballistic Transport in Suspended Graphene. *Nature Nanotechnology* 3: 491-495

Geim, A. K. and K. S. Novoselov. 2007. The Rise of Graphene. *Nature Mater.* 6: 183–191.

Kim H, A. A. Abdala, and C.W. Macosko. 2010. Graphene/Polymer Nanocomposites. *Macromolecules* 43:6515-6530.

Lee, C., X. Wei, J. Kysar, and J. Hone. 2008. Measurement of the Elastic Properties and Intrinsic Strength of Monolayer Graphene. *Science* 321: 385-388.

Lerf, A.; H. He, M. Forster, and J. Klinowski. 1998. Structure of Graphite Oxide Revisited. *J. Phys. Chem. B* 102: 4477–4482.

McAllister M. J., J. L. Li, D. H. Adamson, H. C. Schniepp, A. A. Abdala, J. Liu, M. Herrera-Alonso, D. L. Milius, R. Car, R. K. Prud'homme, I. A. Aksay. 2007. Single Sheet Functionalized Graphene by Oxidation and Thermal Expansion of Graphite. *Chem Mater* 19:4396-4404.

Nair, R. R., P. Blake, A. N. Grigorenko, K. S. Novoselov, T. J. Booth, T. Stauber, N. M. R. Peres, and A. K. Geim. 2008. Fine Structure Constant Defines Visual Transparency of Graphene. *Science* **320**: 1308

Novoselov, K. S.; A. K. Geim, S. V. Morozov, D. Jiang, D. Y. Zhang, S. V. Dubonos, I. V. Grigorieva, A. A. Firsov. 2004. Electric Field Effect in Atomically Thin Carbon Films. *Science* 306: 666–669.

Ramanathan T, A. A. Abdala, S. Stankovich, D. A. Dikin, M. Herrera-Alonso, R. D. Piner, D. H. Adamson, H. C. Schniepp, X. Chen, R. S. Ruoff, S. T. Nguyen, I. A. Aksay, R. K. Prud'Homme, and L. C. Brinson. 2008.

Functionalized Graphene Sheets for Polymer Nanocomposites. *Nat Nanotechnol* 3:327-331.

Stankovich S, D. A. Dikin, G. H. B. Dommett, K. M. Kohlhaas, E. J. Zimney, E. A. Stach, R. D. Piner, S. T. Nguyen, and R. S. Ruoff. 2006. Graphene-based composite materials. *Nature* 442:282-286.

Staudenmaier, L. 1898. Method for the Preparation of Graphitic Acid. *Ber. Dtsch. Chem. Ges.* 31:1481–87.